The Non Linear Behavior of the Microplane Model in COMSOL

A. Frigerio[1]
[1]RSE S.p.A.
*via Rubattino, 54 – 20134 Milan (Italy), antonella.frigerio@rse-web.it

Abstract: Numerical models based on the Finite Element Method (FEM) are frequently used to evaluate the safety conditions of large concrete structures. In the last year, the elastic behavior of the Microplane Model was implemented in COMSOL because it is considered a promising approach able to overcome those limits typical of the classical approaches, which can in general simulate only a few specific characteristics of concrete, but not the overall behavior. The basic idea of the Microplane Model is related to the observation that the main mechanical phenomena of concrete take place on planes whose orientation depends on load and material conditions.
This paper deals with the review of the linear behavior where some remarks are needed and a description of the implementation process within COMSOL of the non-linear behavior of the Microplane Model, based on the definition of boundary surfaces. In order to verify this part, some tests are presented as well.

Keywords: Finite Element Method, concrete mechanical behavior, Microplane Model.

1. Introduction

In the last European COMSOL Conference, held in Stuttgart (Germany) in 2011, [1], the philosophy governing the theory the Microplane Model is based on and a detailed description of the process followed to implement its elastic behavior within COMSOL were presented.

This paper focuses on the further advances from that condition being the formulation of the non-linear behavior of the Microplane Model, [2]÷[9], as well as its implementation within COMSOL introduced and described in detail. First, some remarks regarding how the linear behavior of the Microplane Model works within COMSOL are provided to allow a correct use.

2. The linear behavior: some remarks

2.1 Some hints on the elastic behavior

It is worth briefly recalling the different logical scheme that characterizes the elastic behavior of the Microplane Model with respect to that of classical approaches.

As a convention and consistently with the previous work, in this paper the subscript N stands for the component of the strain/stress vectors that are normal to microplanes, while M and L are referred to the tangential components.
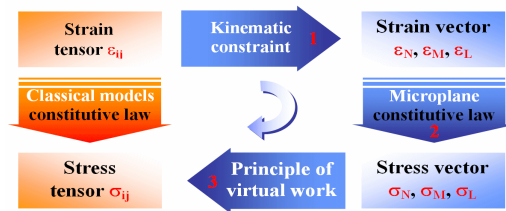

Figure 1. The logical scheme of the elastic behavior of the microplane model (in blue) compared with that of classical approaches (in orange).

Considering the scheme in Figure 1, three steps characterize the elastic behavior of the Microplane Model:

1. considering each material point, the strain vector is computed projecting the strain tensor ε_{ij} on each microplane k, that is applying the kinematic constraint:

$$\varepsilon_i^k = \varepsilon_{ij} n_j \qquad (1)$$

being n_j the unit vector components normal to the microplane k;

2. the stress vectors are computed by means of the elastic incremental relations of the Microplane Model in the rate form:

$$\dot{\sigma}_V = E_V \dot{\varepsilon}_V \; ; \; \dot{\sigma}_D = E_D \dot{\varepsilon}_D \qquad (2a,b)$$

$$\dot{\sigma}_M = E_M \dot{\varepsilon}_M \; ; \; \dot{\sigma}_L = E_L \dot{\varepsilon}_L \qquad (3a,b)$$

where E_V, E_D and E_T are the microplane elastic moduli;

3. the macroscopic stress tensor σ_{ij} is calculated applying the principle of virtual work written with reference to the surface Ω of a unit

hemisphere whose center is the material point:

$$\sigma_{ij} = \frac{3}{2\pi} \int_\Omega \left(\sigma_N \cdot N_{ij} + \sigma_M \cdot M_{ij} + \sigma_L \cdot L_{ij} \right) d\Omega \quad (4)$$

where N_{ij}, M_{ij} and L_{ij} are tensors, [1];

The integral over the surface Ω represents an integration that considers an infinite number of microplanes but, as its solution is not a trivial matter, Gaussian quadrature formulas of various degrees of approximation are adopted:

$$\sigma_{ij} \approx 6 \sum_{k=1}^{N_{mp}} w_k \left(\sigma_N \cdot N_{ij} + \sigma_M \cdot M_{ij} + \sigma_L \cdot L_{ij} \right)^{(k)} \quad (5)$$

In this work, 28 microplanes are considered for each material point (Figure 2) as this choice is deemed a good arrangement between an accurate solution of the integration formula and the computational cost of the overall method in terms of time and numerical resources.
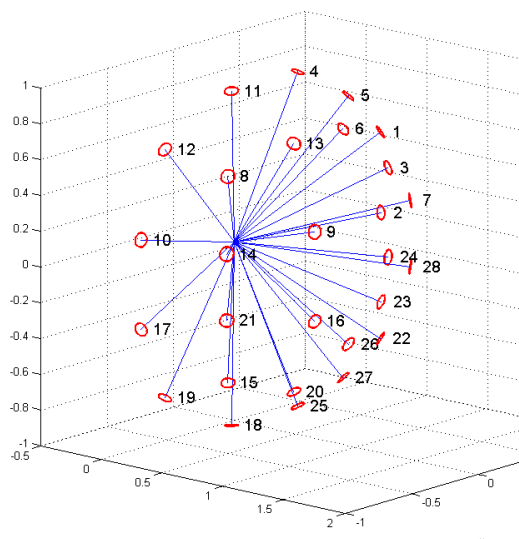

Figure 2. Unit vector components normal to the 28 microplanes assumed in the hemisphere of a material point

2.2 Choice of the Finite Element shape

Last year, the accuracy of the implementation process of the *linear elastic* behavior of the Microplane Model was verified taking into consideration a schematic geometry of a concrete gravity dam, where the dead weight of the structure as well as the hydrostatic pressure of the reservoir were applied [1]. The field of stresses provided by this static analysis was qualitatively in good agreement with that computed applying a conventional linear elastic model, anyway a slight difference was detected in the peak values.

This discrepancy was thoroughly investigated and, finally, it was find out that the problem was not related to the implementation process rather to the choice of the finite element shape. In the *Solid Mechanics* module, the displacement field of each finite element is described by *quadratic* shape functions but, in each PDE module, it is the strain field that has to be characterized by each finite element, thus the use of *linear* shape functions is required. By the light of this need, in addition to the fact that COMSOL adopts a Lagrangian formulation for shape functions, if the mesh is generated by means of *brick* finite elements, the mechanical deformation fields becomes incongruent with respect to that defined into the PDE modules. This incongruence does not happen if *tetrahedral* finite elements are used. To better understand, let's consider 2D linear and quadratic finite elements, whose shape functions have as many polynomial terms as the number of nodes of the finite element (Figure 3).
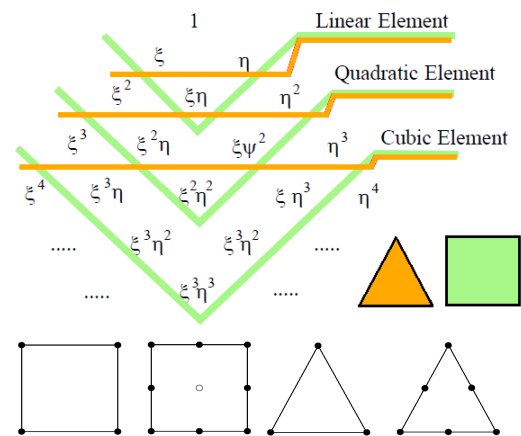

Figure 3. Pascal triangle to define the polynomial terms of finite elements shape functions for a squared and triangle 2D finite element, linear and quadratic

The deformation field, obtained deriving the polynomial quadratic shape function of the displacement field of a *squared* finite element, has some polynomial terms that are not present

in the related linear shape function of the deformation field of the squared finite element of the PDE modules. Making reference to Figure 3, you might assessed that this does not occur anymore in case *triangle* 2D element are used:

$$u = a + bx + cy + dxy + ex^2 + fy^2 \qquad (6)$$

$$\varepsilon_x \left[= \frac{\partial u}{\partial x} \right] = a' + b'x + c'y \qquad (7)$$

The mesh of the concrete gravity dam was therefore modified as shown in Figure 4. The use of tetrahedral finite elements allows verifying the correctness of the implementation process of the linear behavior of the Microplane Model.
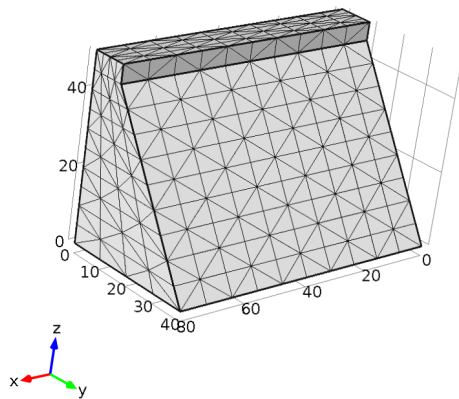

Figure 4. The tetrahedral finite elements used to discretize a schematized concrete gravity dam

3. The non-linear behavior

The non-linear behavior of the Microplane Model is defined by imposing stress-strain boundaries at the microplane level, [2]÷[9]. These boundaries may be regarded as strain-dependent yield limits which can exhibit strain softening. Exceeding these boundaries is never allowed whereas, within the domain they mark out, the material response is incrementally elastic. Movements along these boundaries are permitted only if strain and stress increments are of the same sign, otherwise elastic unloading occurs. Damage may be modeled as well by progressively reducing the elastic moduli of the incremental laws within the elastic domain.

In order to characterize these boundaries, 17 constant material parameters, denoted as c_1, c_2... c_{17}, and 4 free parameters, denoted as k_1, k_2, k_3, k_4, are used. The former parameters may be

taken fixed for all the types of concrete whereas the latter ones may be adjusted to differentiate various concretes. The identification of free parameters can be carried out fitting test data. In this paper, the values reported in Table 1 and Table 2 are assumed respectively for the constant and free parameters.

Table 1: Constant material parameters

c_1	0.62	c_{10}	0.73
c_2	2.76	c_{11}	0.20
c_3	4.00	c_{12}	7000.00
c_4	70.00	c_{13}	0.20
c_5	2.50	c_{14}	0.50
c_6	1.30	c_{15}	0.02
c_7	50.00	c_{16}	0.01
c_8	8.00	c_{17}	0.40
c_9	1.30		

Table 2: Free material parameters

k_1	0.000245	k_3	12
k_2	110	k_4	38

The free values in Table 2 are representative of a concrete which may attain an uniaxial compression strength of 46 MPa, the axial normal strain at peak stress equal to 0.0036, and an elastic modulus of 25 GPa.

Making reference to the *Model Builder* window of COMSOL, all these parameters are placed within the *Global Definitions* node.

In the next paragraphs, the boundaries are briefly described. The normal, volumetric, and deviatoric components of the stress boundary can be assumed to be dependent only on their conjugate strains at the microplane level. Nevertheless, the macroscopic response is well captured thanks to the interactions occurring among microplanes according to the applied kinematic constraints, and thanks to the fact that different microplanes can enter the unloading or reloading phase at different times.

3.1 Tensile normal boundary

The tensile normal boundary is given as:

$$\sigma_N^b = E k_1 c_1 \exp\left(-\frac{\langle \varepsilon_N - c_1 c_2 k_1 \rangle}{k_1 c_3 + \langle -c_4 (\sigma_V / E_V) \rangle} \right) \qquad (8)$$

where subscript b refers to the stress at the boundary. Macaulay brackets stand for: $<Value> = \text{Max}(Value,0)$.
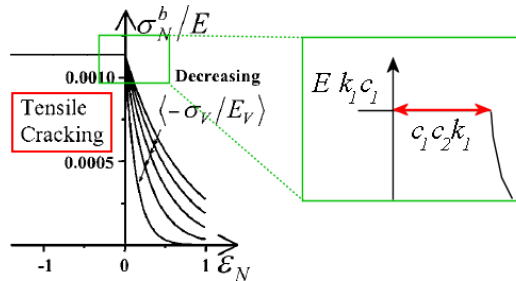

Figure 5. Tensile normal boundary

In particular, this functions is able to define also the horizontal segment of the boundary, representing yield limit, as shown in Figure 5.

Physically, the initial descending part of this boundary describes the tensile cracking parallel to the microplane, whereas its tail defines the frictional pullout of fragments bridging the crack surfaces.

3.2 Volumetric boundaries

The volumetric boundaries are given as:

$$\sigma_V^b = -Ek_1k_3 \exp\left(-\frac{\varepsilon_V}{k_1k_4}\right) \quad \text{for } \sigma_v < 0 \qquad (9)$$

$$\sigma_V^b = \frac{Ek_1c_{13}}{\left[1 + (c_{14}/k_1)\langle\varepsilon_V - k_1c_{13}\rangle\right]^2} \quad \text{for } \sigma_v > 0 \quad (10)$$
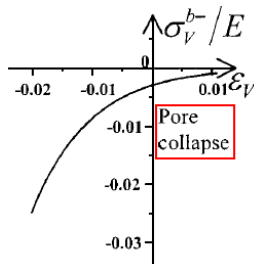

Figure 6. Volumetric boundary in compression

The inelastic behavior under hydrostatic pressure, as well as uniaxial compressive strain, do not exhibit strain softening, but it progressively shows stronger hardening caused primarily by collapse and closure of pores (Figure 6).
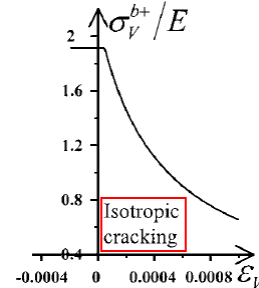

Figure 7. Volumetric boundary in tension

A tensile volumetric boundary is needed too as the normal tensile boundary alone cannot prevent unreasonable lateral strains in post peak softening under uniaxial, unconfined, tension (Figure 7).

3.3 Deviatoric boundaries

The deviatoric boundaries are given as:

$$\sigma_D^b = -\frac{Ek_1c_8}{1 + \left(\langle-\varepsilon_D - c_8c_9k_1\rangle/k_1c_7\right)^2} \quad \text{for } \sigma_D < 0 \quad (11)$$

$$\sigma_D^b = \frac{Ek_1c_5}{1 + \left(\langle\varepsilon_D - c_5c_6k_1\rangle/k_1c_{17}c_7\right)^2} \quad \text{for } \sigma_D > 0 \quad (12)$$
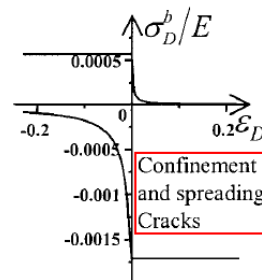

Figure 8. Deviatoric boundaries

The compressive deviatoric boundary controls the axial crushing strain of concrete in compression when lateral confinement is too weak to prevent crushing; instead, the tensile deviatoric boundary simulates the transverse crack opening of axial distributed cracks in compression and controls the volumetric expansion and lateral strains in unconfined compression tests (Figure 8).

3.4 Frictional yield boundary

The frictional yield boundary is given as:

$$\sigma_T^b = \frac{E_T k_1 k_2 c_{10} \left\langle -\sigma_N + \sigma_N^0 \right\rangle}{E_T k_1 k_2 + c_{10} \left\langle -\sigma_N + \sigma_N^0 \right\rangle} \tag{13}$$

being:

$$\sigma_N^0 = \frac{E_T k_1 c_{11}}{1 + c_{12} \left\langle \varepsilon_V \right\rangle} \tag{14}$$

The initial slope of the boundary, close to the origin, is as follows:

$$\left[\frac{d\sigma_T}{d\sigma_N} \right]_{\sigma_N=0} = -c_{10} \tag{15}$$

As the compressive stress magnitude increases, it approaches a horizontal asymptote:

$$lim_{\sigma_N \to -\infty} \sigma_T = E_T k_1 k_2 \tag{16}$$

The existence of a horizontal asymptote means that, at very high confining pressures, concrete becomes a plastic but frictionless material, the friction being characterized by the boundary slope at yield, which tends to zero (Figure 9). When the volumetric strain is small, this boundary provides a finite cohesive stress, which decreases to zero with increasing volumetric strain (Figure 10).
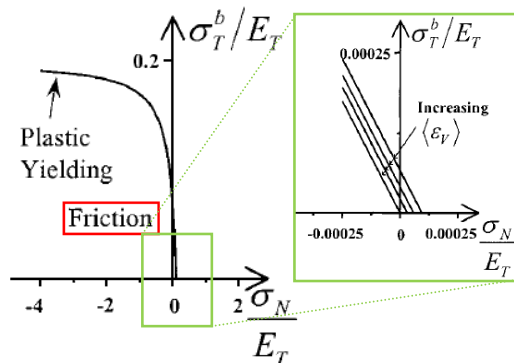

Figure 9. Frictional yield boundary

4. Implementation of the non-linear behavior of the Microplane Model within COMSOL

Considering all the boundaries defined in the previous paragraph, the implementation process will be outlined.

All the following boundaries are defined within the *Global Definitions* node of the *Model Builder* window, into the "*SigmaN*" set, [1].

4.1 Tensile normal boundary

First, some notes on the meaningful names assigned to each variables are needed:
- sNb*kk*: tensile normal boundary on the *kk* microplane related to the current normal strain;
- eN*kk*int: current normal strain;
- sV*kk*: volumetric stress vector on the *kk* microplane computed by means of the incremental constitutive law;
- sN*kk*: current tensile stress on the *kk* microplane imposed equal to sNb*kk* if a greater value is obtained applying the constitutive law;
- sV*kk*: current volumetric stress on the *kk* microplane;
- sD*kk*: current deviatoric stress on the *kk* microplane.

Considering the conventional names of the variables, this boundary was implemented as follows:

```
sNbkk =
Young*k1*c1*exp(-max(eNkkint+
-c1*c2*k1,0.)/(k1*c3+
+max(-c4*(sVckk/EV),0.)))

sNkk =
(eNkkint<=0)*min(sNbkk,sVckk+sDckk)+
+(eNkkint>0)*(sVckk+sDckk>0)*
*min(sNbkk,sVckk+sDckk)
```

In order to validate these formula, a tensile load was applied on one face of a concrete cube with one meter long edge.

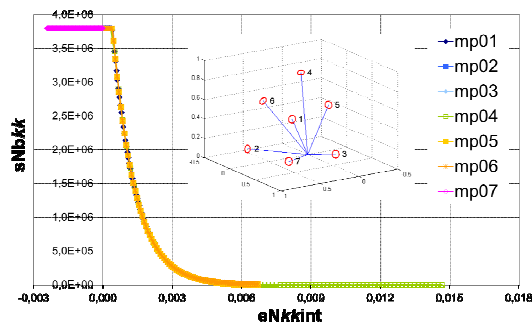The tensile normal boundaries related to the first 7 microplanes are diagrammed in Figure 10.

Figure 10. Tensile normal boundaries on the first 7 microplanes computed by COMSOL

Figure 11. Volumetric stress boundaries on the first 7 microplanes computed by COMSOL

4.2 Volumetric boundaries

The conventional names here used are as follows:

- sVb*kk*n: negative volumetric stress boundary on the *kk* microplane related to the current volumetric strain;
- sVb*kk*p: positive volumetric stress boundary on the *kk* microplane related to the current volumetric strain;
- eV*kk*int: current volumetric strain;
- sVc*kk*: current volumetric stress imposed equal to sVb*kk*n or sVb*kk*p if a greater absolute value is obtained applying the constitutive law;

Considering the conventional names of the variables, these boundaries were implemented as follows:

```
sVbkkn = -Young*k1*k3*
*exp(-eVkkint/(k1*k4))

sVbkkp =  Young*k1*c13/(1+(c14/k1)*
*max(eVkkint-k1*c13,0.))^2

sVckk  =
(sVkk>=0)*min(sVbkkp,sVkk)+(sVkk<0)*
*max(sVbkkn,sVkk)
```

As in the previous case, these formula were verified considering a uniaxial tensile test on a concrete cube. Results in terms of volumetric stress boundaries are shown in Figure 11.
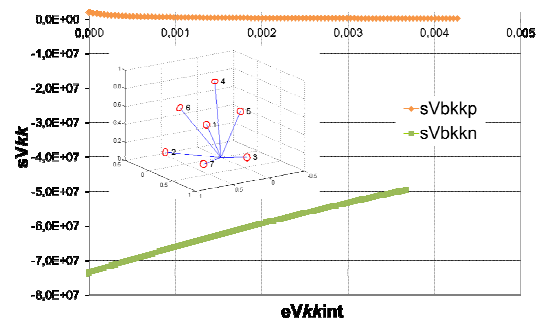
4.3 Deviatoric boundaries

The conventional names here used are as follows:

- sDb*kk*n: negative deviatoric stress boundary on the *kk* microplane related to the current deviatoric strain;
- sDb*kk*p: positive deviatoric stress boundary on the *kk* microplane related to the current deviatoric strain;
- eD*kk*int: current deviatoric strain;
- sDc*kk*: current deviatoric stress imposed equal to sDb*kk*n or sDb*kk*p if a greater absolute value is obtained applying the constitutive law.

Considering the conventional names of the variables, these boundaries were implemented as follows:

```
sDbkkn = -Young*k1*c8/(1+
+(max(-eDkkint+
-c8*c9*k1,0.)/(k1*c7))^2)

sDbkkp =
Young*k1*c5/(1+(max(eDkkint+
-c5*c6*k1,0.)/(k1*c17*c7))^2)

sDckk =
(sDkk>=0)*min(sDbkkp,sDkk)+(sDkk<0)*
*max(sDbkkn,sDkk)
```

Once again, these formula were verified considering a uniaxial tensile test on a concrete cube, and results in terms of deviatoric stress boundaries are shown in Figure 12.
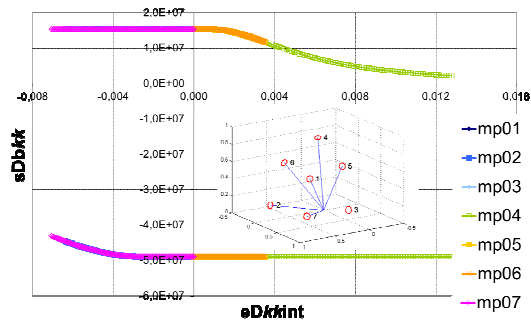
Figure 12. Deviatoric stress boundaries on the first 7 microplanes computed by COMSOL

4.4 Frictional yield boundary

The conventional names used are as follows:

- sNTbkk: frictional yield stress boundary on the kk microplane related to the volumetric strain;
- sTbkk: frictional yield stress boundary on the kk microplane;
- sTkk: current frictional yield stress obtained applying the constitutive law.

Considering the conventional names of the variables, this boundary was implemented as follows:

```
sNTkk =
ET*k1*c11/(1+c12*max(eVkkint,0.))

sTbkk = ET*k1*k2*c10*
*max(-sNkk+sNTkk,0.)/(ET*k1*k2+c10*
*max(-sNkk+sNTkk,0.))

sTkk  =(sMkk^2+sLkk^2)^0.5

sMckk =
if(sTkk>sTbkk,sMkk*sTbkk/sTkk,sMkk)

sLckk =
if(sTkk>sTbkk,sLkk*sTbkk/sTkk,sLkk)
```

5. Conclusions

In this paper some noted are provided in order to allow a correct used of the Microplane Model implemented in COMSOL.

A detailed description of the implementation process followed to implement the non-linear behavior of this model is here addressed. Some examples showing a correct representations of the boundaries that delimited the linear elastic domain are provided. More complex tests are under investigation as they need a proper calibration of the parameters of the Microplane Model in order to represent realistically the mechanical behavior of concrete.

6. References

1. Frigerio, A., The Microplane Model for Concrete in COMSOL, *COMSOL Conference Europe 2011*, Stuttgart - Germany (2011)
2. Taylor, G.I., Plastic strain in metal, *J. Inst. of Metals*, **62**, 307-324 (1938)
3. Bažant, Z.P., Microplane model for strain controlled inelastic behaviour, Chapter 3. *C.S. Desai and R.H. Gallagher eds.*, Wiley, London (1984)
4. Bažant, Z.P. and Oh, B., Microplane model for progressive fracture of concrete and rock, *ASCE Journal of Engineering Mechanics*, **111(4)**, 559-582 (1985)
5. Bažant, Z.P. and Prat, P., Microplane model for brittle-plastic material: I. Theory, *Journal of Engineering Mechanics*, **114(10)**, 1672-1688 (1988)
6. Bažant, Z.P. and Prat, P., Microplane model for brittle-plastic material: II. Verification, *Journal of Engineering Mechanics*, **114(10)**, 1689-1702 (1988)
7. Bažant, Z.P., Xiang, Y. and Prat, P., Microplane model for concrete: I. Stress-strain boundaries and finite strain, *Journal of Engineering Mechanics*, **122(3)**, 245-262 (1996)
8. Bažant, Z.P., Xiang, Y., Adley, M. and Prat, P., Microplane model for concrete: II. Data delocalization and verification, *Journal of Engineering Mechanics*, **122(3)**, 263-268 (1996)
9. Bažant, Z.P. and Carol, I., Damage and plasticity in microplane theory, *International Journal of Solids and Structures*, **34(29)**, 3807-3835 (1997)